ACS Catalysis

Research Article

pubs.acs.org/acscatalysis

Activation of Wild-Type Cytochrome P450BM3 by the Next Generation of Decoy Molecules: Enhanced Hydroxylation of Gaseous Alkanes and Crystallographic Evidence

Zhiqi Cong,[†] Osami Shoji,*[,†] Chie Kasai,[†] Norifumi Kawakami,[‡] Hiroshi Sugimoto, [§] Yoshitsugu Shiro, [§] and Yoshihito Watanabe*[,‡]

[†]Department of Chemistry, Graduate School of Science, and [‡]Research Center for Materials Science, Nagoya University, Furo-cho, Chikusa-ku, Nagoya 464-8602, Japan

[§]RIKEN SPing-8 Center, Harima Institute. 1-1-1 Kouto, Sayo, Hyogo 679-5148, Japan

Supporting Information

ABSTRACT: The direct hydroxylation of alkanes under mild conditions is a key issue in catalytic chemistry that addresses an increasing number of industrial and economic requirements. Cytochrome P450s are monooxygenases that are capable of oxidizing less reactive C−H bonds; however, wild-type P450s are unavailable for many important nonnative substrates such as gaseous alkanes. Here, we report the enhanced hydroxylation activities and crystallographic evidence for the role of decoy molecules in wild-type P450BM3-catalyzed hydroxylation of gaseous ethane and propane by using the next generation of decoy molecule. A cocrystal structure of P450BM3 and a decoy molecule reveals that an *N*-perfluoroacyl amino acid (decoy molecule) partially occupies the substrate-binding site of P450BM3. This binding of the decoy re-forms the active site pocket to allow the accommodation of small substrates and simultaneously influences the formation of compound I species by expelling water molecules from the active site.

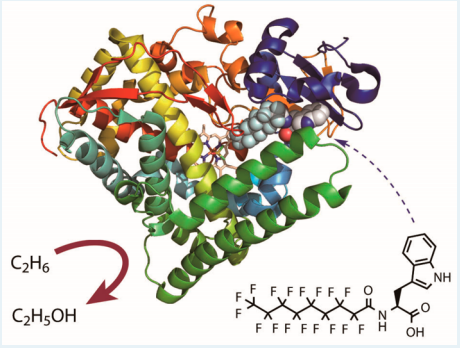

KEYWORDS: *biocatalysis, gaseous alkanes, cytochromes, hydroxylation, decoy molecule*

INTRODUCTION

Gaseous alkanes, which are found in abundance in natural gas, are important fuels and potential chemical feedstock.[1] The development of molecular catalysts (homogeneous and/or heterogeneous) for the selective hydroxylation of less-reactive gaseous alkanes is a longstanding challenge and a current topic of interest, considering increasing industrial and economic requirements.[2,3] One of the main difficulties for gaseous alkane hydroxylation is their high C−H bond-dissociation energies (BDEs). For example, methane and ethane have BDEs of 104.9 and 101.4 kcal/mol, respectively.[4] Although methane monooxygenases from methanotrophic bacteria oxidize methane to methanol under mild conditions, they are not suitable for further application as biocatalysts, mainly because of difficulties associated with preparing the multicomponent system in recombinant form.[5,6] Cytochrome P450s (P450s) are a superfamily of iron-containing monooxygenases that are capable of breaking strong C−H bonds of hydrocarbons. Because recombinant forms of P450s are prepared by using common expression systems such as *Escherichia coli*, P450s have great potential for further engineering and subsequent application in synthetic chemistry.[7−9] Unfortunately, the substrate specificity of cytochrome P450s makes them unsuitable for the hydroxylation of gaseous small alkanes, because P450s, especially those isolated from bacteria, recognize their specific substrates by intermolecular interactions to ensure their specificity and efficiency. For the past few decades, protein engineering has emerged as a powerful tool to remodel P450s for the oxyfunctionalization of nonnative substrates. These studies have succeeded in changing the substrate specificity and have improved the catalytic activity of P450s by the application of rational and semirational structure-based mutagenesis, as well as by directed evolution techniques (random mutagenesis).[10−16] Although challenging, it is still possible to apply wild-type P450s for the oxidation of small nonnative substrates.

In the absence of substrates, the generation of an active intermediate of P450s is prevented by the coordination of a sixth water ligand in the low-spin resting state of the heme iron (substrate-free form).[17] The binding of substrate perturbs the aqua ligand, which leads to a shift of the heme to a high-spin state (substrate-bound form)[18] accompanied by a positive redox potential shift that initiates the reduction of ferric heme (Figure 1A). Subsequent O_2 binding to the ferrous heme followed by its reductive activation generates an iron(IV)−oxo cation radical intermediate (compound I), which is generally considered to be the active species that is responsible for substrate oxidation (Figure 1B).[19,20] According to the oxygen-

Received: October 15, 2014
Revised: November 12, 2014
Published: November 18, 2014

 © 2014 American Chemical Society

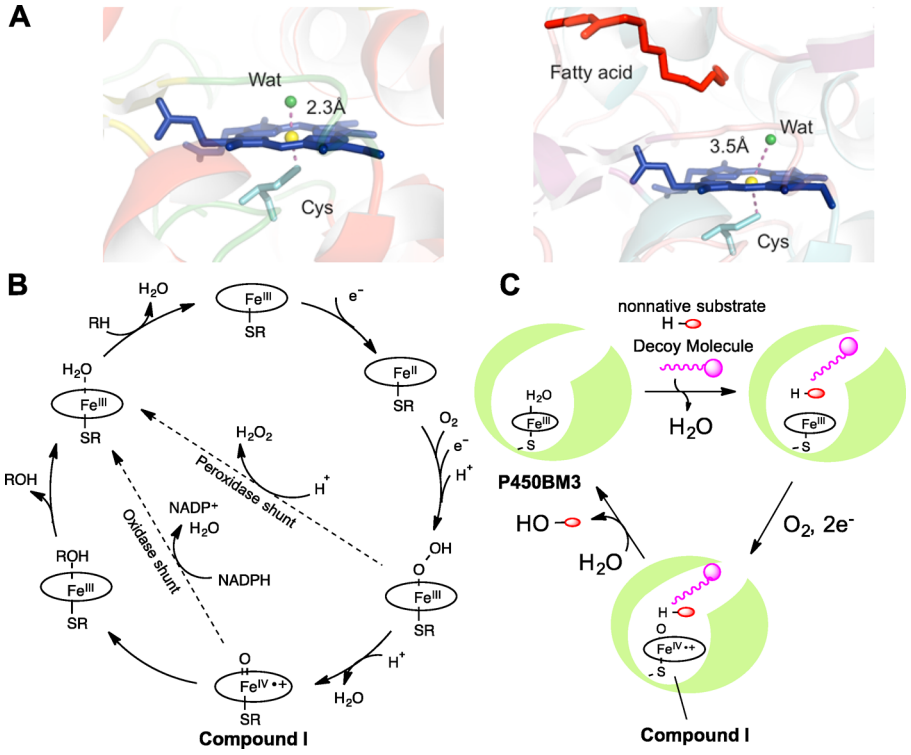

Figure 1. (A) Active site structures of wild-type P450BM3: substrate-free form[17] (left, inactive state, PDB code 2HDP); *N*-palmitoylglycine-bound form[18] (right, active state, PDB code 1JPZ). (B) Catalytic cycle of cytochrome P450. (C) Schematic representation of a plausible catalytic cycle of the "P450BM3-decoy molecule system".

activation mechanism of P450s for the generation of compound I, substrate binding serves as a switch to start the reaction. For example, P450BM3, a fatty acid hydroxylase isolated from *Bacillus megaterium*, selectively binds long-alkyl-chain fatty acids to start its catalytic cycle.[21] Although wild-type P450BM3 shows very high catalytic activity for fatty acid hydroxylation, it does not efficiently catalyze nonnative substrates with structures that are significantly different from those of fatty acids because these nonnative substrates do not bind to the enzyme to initiate the first step of the catalytic cycle (Figure 1C). The crystal structure of a substrate-bound form of P450BM3 shows that the fatty acid (palmitoleic acid) is fixed by two major interactions with P450BM3: (1) a hydrophobic interaction of the alkyl chain of the fatty acid with hydrophobic residues in the active site and (2) hydrogen bonding and electrostatic interaction of the carboxylate in the fatty acid with amino acids Tyr51 and Arg47 located at the entrance to the active site of P450BM3 (Figure 2A).[22] Insertion of the alkyl chain into the active site is critical, because this switches on the reaction by removing the water molecule coordinated to the ferric heme. In fact, carboxylic acids with a short alkyl chain of less than 12 carbon atoms are not hydroxylated by P450BM3.[23] Furthermore, P450BM3 does not start the catalytic hydroxylation of normal alkanes such as tetradecane and hexadecane, which do not have the carboxyl group.[24] This indicates that the interaction of the carboxylate with Arg47 and Tyr51 is also critical for initiating the monooxygenation. This cooperative switching mechanism of the substrate recognition by P450BM3 contributes to its high substrate specificity. Recently, we have demonstrated that the switch of P450s can be turned on by using a series of perfluorinated carboxylic acids (PFCs) with shorter alkyl chains named "decoy molecules" such as perfluorinated nonanoic acid.[25,26] In these cases, P450BM3 misrecognizes PFCs as its natural substrate because their structures resemble those of fatty acids, since the atomic radius of fluorine is similar to that of hydrogen. Thus, PFCs turn on P450s, which adopt the active, high-spin state to start the catalytic cycle (Figure 1C). By utilizing this substrate misrecognition, a variety of substrates such as propane and benzene can be hydroxylated by wild-type P450BM3.[25−28] The catalytic activities for nonnative substrates, however, are still lower than those of long-alkyl-chain fatty acids. We presume the interaction of PFCs with P450BM3 is not sufficient to fully switch on P450BM3 because of its weak binding affinity to the enzyme. However, it was reported that hydroxylation of *N*-palmitoyl glycine is more efficiently catalyzed by P450BM3 than palmitic acid because of an increased association constant of *N*-palmitoyl glycine (K_d = 262 nM).[18] The crystal structure of an *N*-palmitoylglycine-bound form of P450BM3 shows additional hydrogen-bonding interactions of the carboxylate group in *N*-palmitoylglycine with Gln73 and Ala74 (Figure 2B),[18] which are expected to contribute to the improved binding affinity of *N*-palmitoylglycine. These observations allow a new generation of decoy molecules to be developed on the

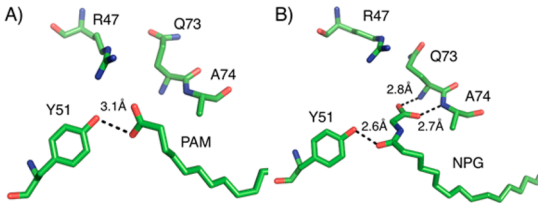

Figure 2. Substrate-binding sites of P450BM3 in complexes with (A) palmitoleic acid (PAM, PDB code 1FAG) and (B) *N*-palmitoylglycine (NPG, PDB code 1JPZ).

dx.doi.org/10.1021/cs501592f | *ACS Catal.* 2015, 5, 150−156

basis of the introduction of an amino acid onto the PFCs (Chart 1). The resulting molecule was anticipated to interact strongly with P450BM3, resulting in higher rates of hydroxylation of small aliphatic and aromatic hydrocarbons.

Chart 1. Design of *N*-Perfluoroacyl Amino Acids as Second-Generation Decoy Molecules Used in This Study

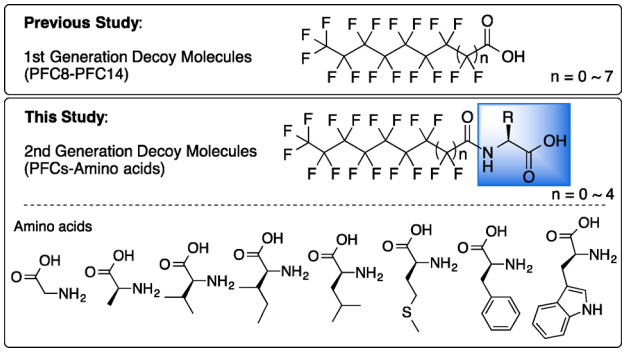

In a mutagenesis study on the oxidation of hydrophobic substrates by P450BM3,[29] the replacement of Arg47 and Tyr51 by hydrophobic amino acids (R47L/Y51F) greatly improved the catalytic activity. The results indicate that a hydrophobic environment at the entrance of the substrate access channel in P450BM3 would be conducive for the hydroxylation of hydrophobic substrates. We thus prepared a series of *N*-perfluoroacyl amino acids with hydrophobic side chains as a new generation of decoy molecules (Chart 1). Herein, we report that *N*-perfluoroacyl amino acids with hydrophobic side chains do indeed strongly activate (arouse) wild-type P450BM3, and we demonstrate that the hydroxylation rates of gaseous alkanes are reached to 45/min/P450 for ethane and 256/min/P450 for propane, by employing *N*-perfluorononanoyl-L-leucine. Furthermore, we have succeeded in obtaining the crystal structure of *N*-perfluorononanoyl L-tryptophan-bound P450BM3, which provides crucial evidence for the roles of decoy molecules and gives some mechanistic insights into the activation of wild-type P450 by decoy molecules and into how gaseous alkanes gain access to the heme pocket.

EXPERIMENTAL SECTION

Decoy Molecules. The preparation, spectroscopic characterization, and dissociation constants of decoy molecules, as well as absorption spectral studies of P450BM3 in the presence of decoy molecules, are described in the Supporting Information.

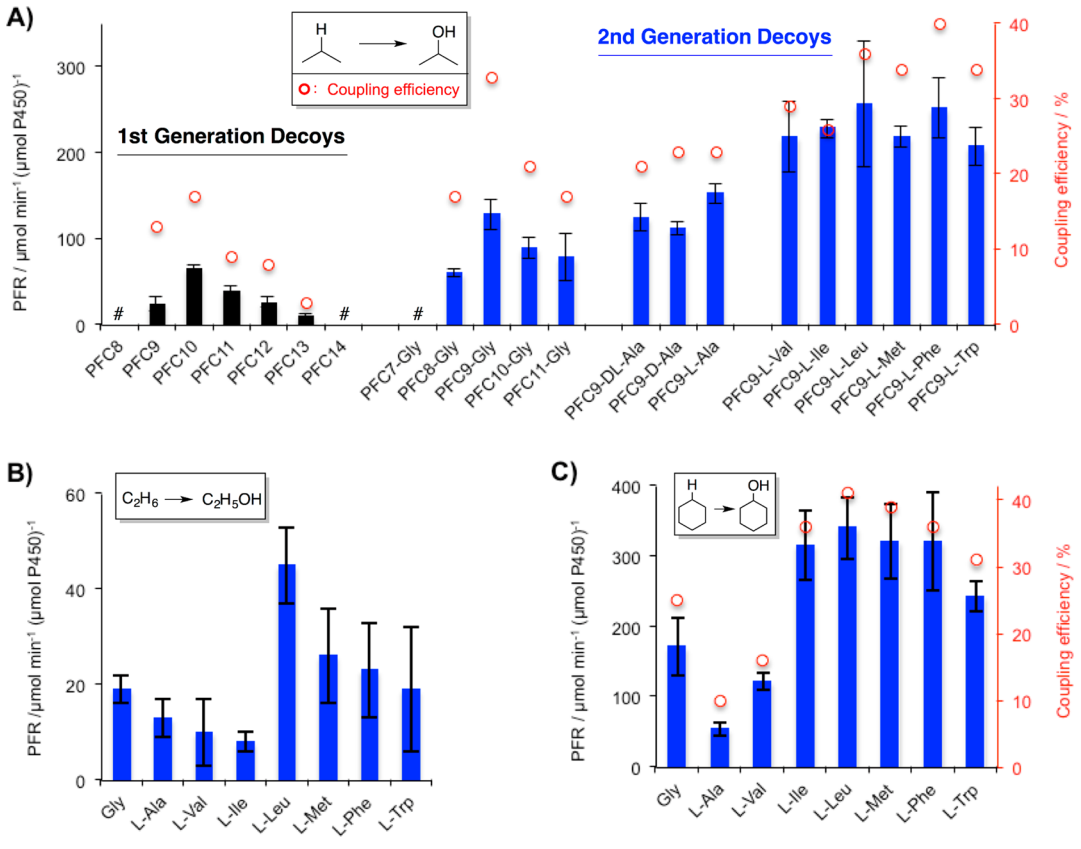

Figure 3. Hydroxylation of propane (A), ethane (B), and cyclohexane (C) catalyzed by wild-type P450BM3 (0.5 μM) with *N*-perfluoroacyl amino acids (100 μM) as second-generation decoy molecules. The previous results from the first-generation decoy molecules (PFCs) are also shown in (A). The # symbols denote the reactions in which the product was not detected. *N*-Perfluorononanoyl amino acids are abbreviated to the three-letter codes of the corresponding amino acids in (B) and (C). For the hydroxylation of propane (A) and cyclohexane (C), 5 mM NADPH was added to the reaction mixture. The ethane hydroxylation was performed by using an NADPH regeneration system consisting of D-glucose (100 mM), $NADP^+$ (1 mM), and glucose dehydrogenase (1 unit). The PFR is given in μmol min^{-1} (μmol of P450)$^{-1}$, and the error bars denote the standard deviation calculated from three parallel experiments. The coupling efficiencies ([product formation]/[NADPH consumption] × 100) are shown as red open circles in (A) and (C).

dx.doi.org/10.1021/cs501592f | ACS Catal. 2015, 5, 150−156

Procedure for Hydroxylation of Propane. To a stirred gas-saturated buffer solution (propane/oxygen 80/20 v/v) composed of 20 mM Tris HCl (pH 7.4) and 100 mM KCl (1 mL) in a glass sample bottle at room temperature were successively added P450BM3 (0.5 μM), a methanolic solution of *N*-perfluoroacyl amino acid (decoy molecule) (100 μM), and NADPH (5 mM). The reactor was immediately fitted with a balloon (propane/oxygen ca. 1/1), and air in the bottle was replaced by the mixed gas for 2 min. After addition of NADPH to start the reaction, the reaction was carried out for 10 min, and then a sample of the reaction mixture (10 μL) was taken to determine the consumption of NADPH. The reaction solution was mixed with sodium nitrite (150 mg), hexane (1 mL), and 3-pentanol (1 mM, internal standard). Aqueous sulfuric acid (20%, 150 μL) was added dropwise to the mixture cooled in an ice bath over 15 min. The organic phase was separated and washed with water, and the obtained solution was directly analyzed by gas chromatography (GC2014; Shimadzu) with an Rtx-1 column (Restek).

The hydroxylations of ethane and cyclohexane performed by using similar procedures are described in detail in the Supporting Information.

Procedure for Hydroxylation of Ethane using an NADPH Regeneration System. To a stirred gas-saturated buffer solution (ethane/oxygen 80/20 v/v) composed of 20 mM Tris HCl (pH 7.4) and 100 mM KCl (1 mL) in a glass sample bottle at room temperature were successively added P450BM3 (0.5 μM), *N*-perfluoroacyl amino acid (decoy molecule) (100 μM), D-glucose (100 mM), $NADP^+$ (1 mM), and glucose dehydrogenase (1 unit). The reactor was immediately fitted with a balloon (ethane/oxygen ca. 1/1), and the reaction was carried out under balloon pressure for 4 min. The reaction solution was mixed with sodium nitrite (150 mg), hexane (1 mL), and 3-pentanol (1 mM, internal standard), and then the mixture was carefully treated by addition of diluted sulfuric acid (20%, 150 μL) cooled in an ice bath. After more than 15 min, the organic phase was separated and washed with water. The obtained solution was directly analyzed by gas chromatography (GC2014; Shimadzu) with an Rtx-1 column (Restek). Control experiments were carried out with nitrogen gas instead of ethane under the same conditions.

Crystallization of P450BM3 with *N*-Perfluorononanoyl-L-Tryptophan. The buffer of the purified P450BM3 was exchanged with 50 mM Tris-HCl (pH 7.4) containing 100 μM of *N*-perfluorononanoyl-L-tryptophan and 1% (v/v) dimethyl sulfoxide. P450BM3 was then concentrated to 20.3 mg/mL by centrifugation using Amicon Ultra filter units (Millipore,Co.). An aliquot of the concentrated P450BM3 solution (1 μM) was mixed with 1 μM of a reservoir solution composed of 100 mM Tris-HCl (pH 8.5), 210 mM MgCl, and 21% (w/v) PEG8000. The cocrystals were grown by a sitting-drop vapor diffusion method at 20 °C for 20 days.

Data Collection and Refinement. Crystals were flash-cooled by liquid nitrogen. X-ray diffraction data sets were collected on the beamline BL26B2 equipped with a MAR225 CCD detector at SPring-8 (Hyogo, Japan) with a 1.0 Å wavelength at 100 K. The program HKL2000[30] was used for integration of diffraction intensities and scaling. The structure was solved by molecular replacement with MolRep.[31] The structure of P450BM3 with *N*-palmitoylmethionine (1ZO9) was used as a search model. Model building and refinement were performed by using COOT[32] and REFMAC5.[33] The *N*-perfluorononanoyl-L-tryptophan model was generated by using a Dundee PRODRG server[34] and used in the refinement with COOT and REFMAC5. All protein figures were depicted by using PyMOL.[35] The final refinement statistics are summarized in Table S1 (Supporting Information).

RESULTS AND DISCUSSION

A series of *N*-perfluoroacylglycines with different lengths of alkyl chain (PFC6-Gly to PFC11-Gly) were synthesized both to examine the effect of the glycine on propane hydroxylation and to establish an appropriate length for the alkyl chain of the *N*-perfluoroacyl amino acids (Figure 3A and pages S1–S4 in the Supporting Information).[36] As expected, the catalytic hydroxylation activity and the binding affinity (Table 1) were both drastically improved by simply introducing glycine. The optimum chain length was PFC9, and the use of this compound gave a product formation rate (PFR) of 2-propanol of 128/min/P450 (Figure 3A). To examine the effect of the side chain structure and chirality of the amino acid on propane hydroxylation, we prepared a series of PFC9 derivatives modified with amino acids bearing a range of hydrophobic side chains (Chart 1, Figure 3A, and pages S1–S4 in the Supporting Information). Among the *N*-perfluorononanoyl amino acids examined, *N*-perfluorononanoyl-L-leucine was the most effective for propane hydroxylation (PFR = 256/min/P450, Figure 3A). This activity reaches about half of that obtained by the best reported mutant of P450BM3 (propane monooxygenases, $P450_{PMO}$) with 22 mutations from 15 rounds of directed evolution (455/min/P450) (Figure S5 and Tables S2–S5, Supporting Information),[37] whereas two PFRs obtained under different conditions could not be compared directly. This activity of PFC9-L-Leu for propane hydroxylation was 4 times higher than that of PFC10 (67/min/P450, Figure 3A).[25] The coupling efficiency of PFC9-L-Leu (36%) for propane hydroxylation was increased 2 times in comparison with that of PFC10 (18%),[25] but it was lower than that of $P450_{PMO}$ (94%).[37] The higher affinity could be one of the possible reasons for the higher rates of the hydroxylation reaction. It is interesting to note that compounds with the L-amino acid were better than those with the D enantiomer (Figure 3A and Table S3, Supporting Information). PFC9 derivatives modified by L-amino acids with larger side chains showed a tendency to give higher PFRs (more than 200/min/P450), which suggested a

Table 1. Dissociation Constants of Decoy Molecules Bound to P450BM3

second generation[a]	K_d/μM	first generation[b]	K_d/μM
PFC7-Gly	911		
PFC8-Gly	95	PFC8	1900
PFC9-Gly	22	PFC9	980
PFC10-Gly	3	PFC10	290
PFC11-Gly	5	PFC11	91
PFC9-L-Ala	26	PFC12	30
PFC9-L-Val	7.3	PFC13	1.8
PFC9-L-Ile	4.1	PFC14	13
PFC9-L-Leu	39		
PFC9-L-Met	20		
PFC9-L-Phe	3.4		
PFC9-L-Trp	1.6		

[a]This study. The K_d values of PFC9-DL-Ala and PFC9-D-Ala were not estimated because of the irregular spectral change during titration experiments. [b]Previous study.[25]

dx.doi.org/10.1021/cs501592f | ACS Catal. 2015, 5, 150–156

significant steric effect of the side chain of the amino acid (Figure 3A and Table S4, Supporting Information). Moreover, a small amount of 1-propanol (23/min/P450) was detected under these conditions (Tables S2–S5, Supporting Information), whereas the hydroxylation of the unreactive primary sp^3 C–H bond was observed with P450BM3 and PFCs only when a high pressure of propane was applied (Figure S5, Supporting Information)[27] or when the reaction was performed by using engineered P450BM3 and $P450_{cam}$ (Figure S8, Supporting Information).[38−40]

The hydroxylation of ethane was then examined under similar conditions by using NADPH. Because control experiments using nitrogen gas instead of ethane showed a small amount of ethanol formation due to a side reaction, we calculated the formation rate of ethanol by ethane hydroxylation (4–15/min/P450) after subtracting the background ethanol (Figure S6 and Table S6, Supporting Information). The rates were 6–22 times faster than that of the reaction performed under high-pressure ethane (500 kPa) using PFC10 as the decoy molecule (0.67/min/P450)[27] and were 10–37 times faster than that obtained with the P450BM3 variant ($P450_{PMO}$, 0.4/min/P450).[39] It is not clear at this time how the background ethanol was formed; however, decomposition of NADPH could afford ethanol. Therefore, we also examined ethane hydroxylation by employing a glucose dehydrogenase promoted NADPH regeneration system to reduce the concentration of NADPH in situ.[41] The regeneration system also promoted ethane hydroxylation, with a PFR range of 8–45/min/P450 (Figure 3B and Figure S7 and Table S7, Supporting Information). PFC9-L-Leu gave the largest PFR (45/min/P450), and this activity was comparable with that obtained with the best reported P450 variant (four mutations of P450cam, 78.2/min/P450) for ethane hydroxylation (Figure S8, Supporting Information).[38] In addition, a long-term reaction of ethane hydroxylation was carried out for 5 h in the presence of PFC9-L-Leu together with an NADPH regeneration system to give a TON of 292 μmol/(μmol of P450), which is lower than that observed by $P450_{PMO}$.[39] The hydroxylation of cyclohexane was also examined by using the second generation of decoy molecules, resulting in PFRs higher than those obtained by using the first-generation decoy molecules (Figure 3C).[25]

The high affinity of this series of *N*-perfluoroacyl amino acids to P450BM3 (Table 1 and Figures S13 and S14, Supporting Information) encouraged us to prepare cocrystals of P450BM3 and *N*-perfluoroacyl amino acids. As a result, we succeeded in crystallizing a PFC9-L-Trp-bound form of P450BM3 and obtained crystals that diffracted at 1.8 Å resolution (Figure 4A). In the fatty acid binding channel of P450BM3, clear electron density that was readily assignable to PFC9-L-Trp was observed, and the fluorine atoms were clearly distinguished from proton atoms of fatty acids (Figure 4B and Figure S9, Supporting Information). PFC9-L-Trp was bound to P450BM3 through hydrogen bond interactions with three amino acids: Tyr51, Gln73, and Ala74 (Figure 4B). The overall structure has a quasi-open conformation that is between the open conformation (substrate-free, PDB code 2HPD)[17] and the closed substrate-bound conformations (PDB codes 1FAG (palmitoleic acid),[22] 1JPZ (*N*-palmitoylglycine),[18] and 1ZO9 (*N*-palmitoylmethionine)[42]). Clear changes in the quasi-open conformation from the open conformation of 2HPD are found in the F and G helices and the F/G loop (Figure S10A, Supporting Information). Large differences in comparison with

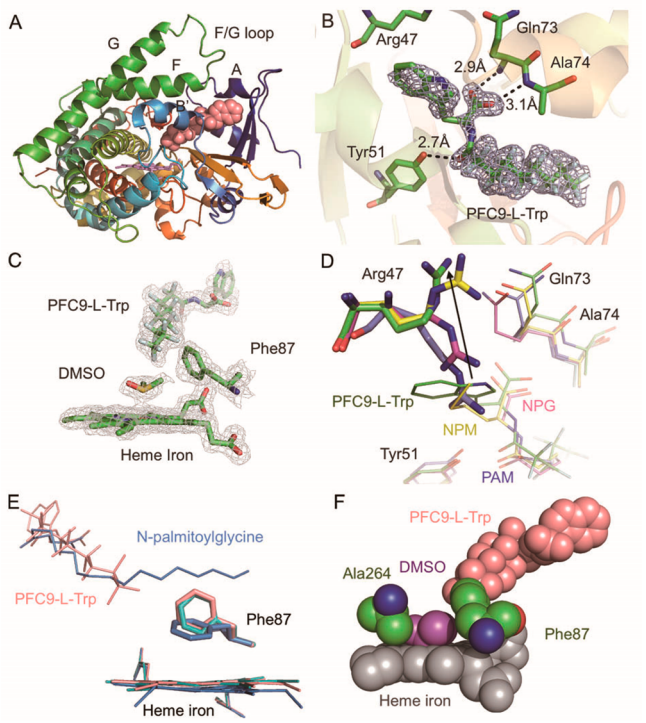

Figure 4. (A) Crystal structure of P450BM3 with PFC9-L-Trp (red sphere). (B) Binding modes of PFC9-L-Trp to P450BM3. An $F_o - F_c$ electron density map contoured at the 3.0 level omitting PFC9-L-Trp is shown in light blue mesh. (C) The $2F_o - F_c$ electron-density map around the active-site pocket. (D) Substrate-induced rotation of Arg47 in an increasing order of PAM- (palmitoleic acid, light blue), NPG- (*N*-palmitoylglycine, magenta), NPM- (*N*-palmitoylmethionine, yellow), and PFC9-L-Trp-bound P450BM3 (green);. (E) Conformational change of Phe87 in substrate-free P450BM3 (cyan), PFC9-L-Trp-bound P450BM3 (pink), and NPG-bound P450BM3 (sky blue). (F) DMSO-bound structure.

the bound forms of P450BM3 were also observed in the I, H, and B′ helices and related loops (Figure S10B, Supporting Information). More importantly, the quasi-open conformation provides space that allows access to an additional small substrate. Furthermore, a DMSO molecule unambiguously occupied the sixth ligand position of the heme instead of a water molecule, according to a $2F_o - F_c$ electron density map contoured at 1σ around this region (Figure 4C), even though only 1% DMSO was present (to improve the solubility of PFC9-L-Trp). The distance between the sulfur atom of DMSO and the heme iron is 2.4 Å (Figure S11A, Supporting Information).[43] This DMSO is also close to PFC9-L-Trp (4.2 Å), Phe87 (3.9 Å), Ala264 (3.2 Å), Thr268 (3.1 Å), and Ala328 (3.8 Å) (Figure S11B, Supporting Information). Considering the similar size of DMSO and small alkanes, this result provides evidence that the short chain length of PFC9-L-Trp allows accommodation of the target substrates near the heme iron. Interestingly, water molecules, which are usually observed near the active center upon binding of long chain fatty acids (1JPZ and 1ZO9), are not observed, possibly because of the increased hydrophobic interaction of decoy molecules with the substrate-binding channel upon the introduction of fluorine (Figure S12, Supporting Information). The results are consistent with the observation that the binding of decoy molecules leads to an increased proportion of high-spin heme iron; thus, the

dx.doi.org/10.1021/cs501592f | ACS Catal. 2015, 5, 150–156

reduction of ferric heme is expected to take place readily in the presence of NADPH.[44]

Conformation changes of key residues in the PFC9-L-Trp-bound P450BM3 provide clear evidence for the transition from a resting state of P450BM3 (substrate free) to a "substrate-bound-like" state upon binding of the decoy molecule. One striking difference between the decoy molecule bound form and the native substrate bound forms is found for Arg47, which is a polar residue close to the entrance of the substrate access channel. This residue moves toward the surface of the protein and away from the substrate (Figure 4D), which may allow the admission of a small substrate. Moreover, a hydrophobic side chain of the decoy molecule occupies the space provided by the rotation of Arg47. Therefore, the water network environment in the entrance of the substrate-binding channel might be disturbed, which makes the entrance more hydrophobic.[42] A second significant change was observed in Phe87, a key residue in the active site, which is 75° inclined to the heme plane, whereas the DMSO binding may also contribute to this orientation (Figures 4C). This perpendicular orientation is similar to that observed in the substrate-free structure (2HPD) but differs from the parallel orientation found in the *N*-palmitoyl glycine-bound structure (1JPZ) (Figures 4E). The perpendicular orientation of Phe87 reduces steric conflict with the bound DMSO (Figure 4F). Because the structure of DMSO-bound P450BM3 could be regarded as a model structure of small alkane-bound P450BM3, the perpendicular orientation of Phe87 would contribute to the accommodation of small alkanes between Phe87 and Ala264. The crystal structure analysis also reveals why the medium chain length of the decoy molecule was effective, while decoy molecules having longer alkyl chains showed better binding affinity to P450BM3. The crystal structure of the PFC9-L-Trp-bound form of P450BM3 indicated that the terminal perfluoromethyl group of PFC9-L-Trp was close to DMSO (4.2 Å, Figure S11B, Supporting Information) coordinated to the heme iron. This observation clearly indicates that, in the case of decoy molecules with alkyl chains longer than nine carbon atoms such as PFC10-L-Leu and PFC11-L-Leu, the binding site for gaseous alkane would be occupied by the alkyl chain of decoy molecules or the access of gaseous alkane would be disturbed by the alkyl chain of decoy molecules, both of which would lead to lower catalytic activities and higher uncoupling reactions (Table S5, Supporting Information),[45] while the binding affinities of PFC10-L-Leu and PFC11-L-Leu are higher than that of PFC9-L-Leu.

CONCLUSION

In conclusion, we have demonstrated that *N*-perfluoroacyl amino acids strongly activate wild-type P450BM3 for the hydroxylation of inert alkanes. PFC9-L-Leu gave PFRs for the hydroxylation of secondary and primary C−H bonds of alkanes that were comparable with those of the best P450 variants prepared by multiple-round mutagenesis. The crystal structure of the PFC9-L-Trp-bound form of P450BM3 revealed the active site re-formation and provided mechanistic insight into the activation of wild-type enzyme by decoy molecules. We conclude that the catalytic activity for gaseous alkane hydroxylation by wild-type P450BM3 would be improved further by optimizing the structure of the decoy molecule. Although we have focused herein on natural amino acids for the modification of the carboxylate group of PFCs, non-natural amino acids may further improve the catalytic activity. Further modification of the amino acids to elongate the terminal of PFCs is also expected to improve the binding affinity as well as the solubility of decoy molecules.

ASSOCIATED CONTENT

Supporting Information

The following file is available free of charge on the ACS Publications website at DOI: 10.1021/cs501592f.

Materials, instruments, and experimental details, Figures S1−S16, and Tables S1−S9 (PDF)

AUTHOR INFORMATION

Corresponding Authors

*E-mail for O.S.: shoji.osami@a.mbox.nagoya-u.ac.jp.
*E-mail for Y.W.: p47297a@nucc.cc.nagoya-u.ac.jp.

Notes

The authors declare no competing financial interest.

ACKNOWLEDGMENTS

This work was supported by a Grant-in-Aid for Scientific Research (S) to Y.W. (24225004), Grants-in-Aid for Scientific Research on Innovative Areas "Molecular Activation Directed toward Straightforward Synthesis" to Y.S. (22105012) and to O.S. (25105724), and a Grant-in-Aid for Young Scientists (A) to O.S. (21685018) from the Ministry of Education, Culture, Sports, Science, and Technology (MEXT) of Japan. We thank Dr. Go Ueno, Dr. Yuki Nakamura, and Dr. Hironori Murakami for their assistance with the data collection at SPring-8.

REFERENCES

(1) Rostrup-Nielsen, J. R. In *Sustainable Strategies for the upgrading of natural gas: fundamentals, challenges, and opportunities*; Derouane, E., Parmon, V., Lemos, F., Ribeiro, F. R., Eds.; Springer: Dordrecth, The Netherlands, 2005.
(2) Hashiguchi, B. G.; Konnick, M. M.; Bischof, S. M.; Gustafson, S. J.; Devarajanm, D.; Gunsalus, N.; Ess, D. H.; Periana, R. A. *Science* **2014**, *343*, 1232−1237.
(3) Labinger, J. A.; Bercaw, J. E. *Nature* **2002**, *417*, 507−514.
(4) Luo, Y. R. *Handbook of bond dissociation energies in organic compounds*; CRC Press: New York, 2003.
(5) Balasubramanian, R.; Smith, S. M.; Rawat, S.; Yatsunyk, L. A. *Nature* **2010**, *465*, 115−119.
(6) Tinberg, C. E.; Lippard, S. J. *Acc. Chem. Res.* **2011**, *44*, 280−288.
(7) Nelson, D. R. *Hum. Genomics* **2009**, *4*, 59−65.
(8) Ortiz de Montellano, P. R. *Cytochrome P450: structure, mechanism, and biochemistry*, 3rd ed.; Kluwer Academic/Plenum Publishers: New York, 2005.
(9) Ortiz de Montellano, P. R. *Chem. Rev.* **2009**, *110*, 932−948.
(10) Petrik, I. D.; Liu, J.; Lu, Y. *Curr. Opin. Chem. Biol.* **2014**, *19*, 67−75.
(11) Ueno, T., Watanabe, Y. *Coordination chemistry in protein cages: principles, design and applications*; Wiley: Hoboken, NJ, 2013.
(12) Narayan, A. R. H.; Sherman, D. H. *Science* **2013**, *339*, 283−284.
(13) Caswell, J. M.; O'Neill, M.; Taylor, S. J.; Moody, T. S. *Curr. Opin. Chem. Biol.* **2013**, *17*, 271−275.
(14) Coelho, P. S.; Brustad, E. M.; Kannan, A.; Arnold, F. H. *Science* **2013**, *339*, 307−310.
(15) Kille, S.; Zilly, F. E.; Acevedo, J. P.; Reetz, M. T. *Nat. Chem.* **2011**, *3*, 738−743.
(16) Zhang, K.; Shafer, B. M.; Demars, M. D., II; Stern, H. A.; Fasan, R. *J. Am. Chem. Soc.* **2012**, *134*, 18695−18704.
(17) Ravichandran, K. G.; Boddupalli, S. S.; Hasemann, C. A.; Peterson, J. A.; Deisenhofer, J. *Science* **1993**, *261*, 731−736.
(18) Haines, D. C.; Tomchick, D. R.; Machius, M.; Peterson, J. A. *Biochemistry* **2001**, *40*, 13456−13465.

(19) Rittle, J.; Green, M. T. *Science* **2010**, *330*, 933−937.
(20) Schlichting, I.; Berendzen, J.; Chu, K.; Stock, A. M.; Maves, S. A.; Benson, D. E.; Sweet, R. M.; Ringe, D.; Petsko, G. A.; Sligar, S. G. *Science* **2000**, *287*, 1615−1622.
(21) Whitehouse, C. J. C.; Bell, S. G.; Wong, L. L. *Chem. Soc. Rev.* **2012**, *41*, 1218−1260.
(22) Li, H.; Poulos, T. L. *Nat. Struct. Biol.* **1997**, *4*, 140−146.
(23) Boddupalli, S. S.; Estabrook, R. W.; Peterson, J. A. *J. Biol. Chem.* **1990**, *265*, 4233−4239.
(24) Miura, Y.; Fulco, A. *Biochim. Biophys. Acta* **1975**, *388*, 305−317.
(25) Kawakami, N.; Shoji, O.; Watanabe, Y. *Angew. Chem., Int. Ed.* **2011**, *50*, 5315−5318.
(26) Zilly, F. E.; Acevedo, J. P.; Augustyniak, W.; Deege, A.; Hausig, U. W.; Reetz, M. T. *Angew. Chem., Int. Ed.* **2011**, *50*, 2720−2724; *Angew. Chem., Int. Ed.* **2013**, *52*, 13503 (corrigendum about the system being unavailable for methane oxidation but available for propane oxidation) .
(27) Kawakami, N.; Shoji, O.; Watanabe, Y. *Chem. Sci.* **2013**, *4*, 2344−2348.
(28) Shoji, O.; Kunimatsu, T.; Kawakami, N.; Watanabe, Y. *Angew. Chem., Int. Ed.* **2013**, *52*, 6606−6610.
(29) Carmichael, A. B.; Wong, L. L. *Eur. J. Biochem.* **2001**, *268*, 3117−3125.
(30) Otwinowski, Z.; Borek, D.; Majewski, W.; Minor, W. *Acta. Crystallogr. A* **2003**, *59*, 228−234.
(31) Vagin, A.; Teplyakov, A. *J. Appl. Crystallogr.* **1997**, *30*, 1022−1025.
(32) Emsley, P.; Cowtan, K. *Acta Crystallogr., Sect. D* **2004**, *60*, 2126−2132.
(33) Murshudov, G. N.; Skubak, P.; Lebedev, A. A.; Pannu, N. S.; Steiner, R. A.; Nicholls, R. A.; Winn, M. D.; Long, F.; Vagin, A. A. *Acta Crystallogr., Sect. D* **2011**, *67*, 355−367.
(34) Schttelkopf, A. W.; van Aalten, D. M. *Acta Crystallogr. Sect. D* **2004**, *60*, 1355−1363.
(35) DeLano, W. L. *The Pymol Molecular Graphics System*; http://www.pymol.org.
(36) Watanabe, H., Fushihoshi, H., Ishida, S. (Fujifilm Co., JPN). Preparation of perfluorocarboxylic derivatives. JP5-279307, October 26, 1993.
(37) Fasan, R.; Chen, M. M.; Crook, N. C.; Arnold, F. H. *Angew. Chem., Int. Ed.* **2007**, *46*, 8414−8418.
(38) Xu, F.; Bell, S. G.; Lednik, J.; Insley, A.; Rao, Z.; Wong, L. L. *Angew. Chem., Int. Ed.* **2005**, *44*, 4029−4032.
(39) Fasan, R.; Meharenna, Y. T.; Snow, C. D.; Poulos, T. L.; Arnold, F. H. *J. Mol. Biol.* **2008**, *383*, 1069−1080.
(40) Chen, M. M.; Coelho, P. S.; Arnold, F. H. *Adv. Synth. Catal.* **2012**, *354*, 964−968.
(41) Weckbecker, A., Hummel, W. *Microbial Enzymes and Biotransformations*; Humana Press: New York, 2005; Vol. *17*, pp 225−238.
(42) Hegde, A.; Haines, D. C.; Bondlela, M.; Chen, B.; Schaffer, N.; Tomchick, D. R.; Machius, M.; Nguyen, H.; Chowdhary, P. K.; Stewart, L.; Lopez, C.; Peterson, J. A. *Biochemistry* **2007**, *46*, 14010−14017.
(43) Matteis, F. D.; Ballou, D. P.; Coon, M. J.; Estabrook, R. W.; Haines, D. C. *Biochem. Pharmacol.* **2012**, *84*, 374−382.
(44) Spectral titrations indicate that *N*-perfluoroacyl amino acids bind to P450 with higher affinity in comparison to that of PFCs, as evidenced by the estimated dissociation constants (Table 1 and Figures S13 and S14, Supporting Information).[25] For example, a small amount of the heme iron in the high-spin state is observed upon addition of decoy molecules (ca. 7% for PFC9-gly), and the ratio of the high-spin heme iron increases to ca. 12% in the presence of cyclohexane (Figure S15, Supporting Information). A ferrous CO complex is formed when NADPH is added to a CO-saturated buffer solution containing P450BM3 and *N*-perfluoroacyl amino acids. These results suggest that tight binding of decoy molecules induces the change of the spin state, followed by the reduction of ferric heme and subsequent binding of an oxygen molecule to initiate the formation of compound I (Figure S16, Supporting Information).
(45) Kuper, J.; Wong, T. S.; Roccatano, D.; Wilmanns, M.; Schwaneberg, U. *J. Am. Chem. Soc.* **2007**, *129*, 5786−5787.